

# On the Influence of Mixed Wettability on the Simulation of Multi-Phase Transport Properties of Core Samples

J.-O. Schwarz<sup>1</sup>, S. Linden<sup>1,2</sup>, J. Becker<sup>1</sup>, C. Wagner<sup>1</sup>, A. Wiegmann<sup>1</sup>

<sup>1</sup>Math2Market GmbH, 67657 Kaiserslautern, Germany

<sup>2</sup>Fraunhofer ITWM, 67663 Kaiserslautern, Germany

*This paper was prepared for presentation at the International Symposium of the Society of Core Analysts held in Snowmass, Colorado, USA, 21-26 August 2016*

## ABSTRACT

The determination of transport properties of reservoir rocks in laboratories is difficult and time-consuming. Therefore there interest is increasing in predicting relative permeability by pore-scale simulations. The wettability of the rock forming minerals is a well-known phenomenon of natural samples that represents a challenge for numerical simulations of rock properties. Through recent innovations, this challenge can be met by our digital rock physics software GeoDict. Comparison of simulations of the relative permeability with and without mixed wettability for a Berea sandstone exhibit clear differences. The most striking difference is the different crossover points between  $k_{r,w}$  and  $k_{r,o}$ . Because this point is a good first indicator for the amount of recoverable oil, the incorporation of mixed wettability in relative permeability simulations is crucial for getting realistic multiphase transport properties from numerical simulations.

## INTRODUCTION

In reservoir engineering multiphase flow in porous media is mainly described by parameters such as porosity  $\phi$ , (absolute) permeability  $K$ , fluid viscosities  $\mu_i$ , the capillary pressure  $p_c$  vs saturation  $S_w$  function and the relative permeability  $k_r$  [1]. The relative permeability vs. saturation function together with absolute permeability has a large influence on the flux of fluid phases. Relative permeability can largely vary depending on rock type, wettability and other parameters. At the same time, experimental determination of relative permeability is difficult and time-consuming. Therefore over the last decade interest has been increasing in predicting relative permeability by pore-scale simulation [2]. GeoDict, the digital rock physics software produced by the Math2Market GmbH, computes relative permeability directly on the pore space as identified by X-ray computed tomography (XCT) by a quasi-static approach that employs the pore morphology method [3,4,5].

Pore morphology (PM) methods determine the capillary pressure – saturation curve of a porous media [3,5]. They are based on modelling the three-dimensional geometric distribution of the fluid phases in the pore space. PM methods are in wide use but were originally limited to a single contact angle ( $\theta$ ). This restriction does not allow for the

complexity of core samples, because the different  $\theta$  of the mineral phases (mixed wettability) influence the distribution of the fluid phases and their potential path ways through the pore space. Recently, this limitation was overcome and demonstrated in 2d for highly porous materials [6]. Our consideration of multiple  $\theta$  (i.e. mineral specific  $\theta$ ) in 3d allows for a realistic modelling of core samples. The multiple  $\theta$  PM method was implemented in GeoDict recently. In this study it is applied to a core sample of a Berea sandstone and the results of these PM calculations are compared to constant  $\theta$  PM calculations for primary drainage.

## **METHODS**

Digital rock physics (DRP) are employed to simulate the multi-phase transport properties of a core sample. The general DRP workflow of scanning the sample by XCT, image-processing of the scan and simulation of the physical rock properties is followed.

### **XCT scanning and sample**

The sample and raw data for this study derive from one of our former studies [7]. Here we use the Berea sandstone sample and its synchrotron-based XCT raw data obtained at the TOMCAT beamline at the Swiss Light Source (Paul Scherrer Institute, Villigen, Switzerland) provided along with that study.

### **Image processing**

The XCT raw data from the benchmark study is further processed with GeoDict to prepare the data for the numerical simulations. The XCT scan is filtered by a Non-local means filter and artifacts are removed by dilation and erosion operations. The different mineral phases in the sample are subsequently segmented by a threshold segmentation. Quartz and feldspar expose an identical range of grey values and could not be separated in that way. However, both minerals exhibit different structures due to the decay of feldspar to clay minerals. This structural difference can be detected by a combination of erosion and dilation algorithms. This feature is used for the differentiation between quartz and feldspar in the final segmentation. See figure 1.

### **Relative permeability**

The relative permeability for the Berea sandstone is simulated in a three step workflow explained in the following. In GeoDict this workflow is fully automated.

### **Absolute permeability**

In a first step the absolute permeability of the Berea sample is computed on the segmented pore space assuming that it is completely saturated with one fluid phase. Absolute permeability ( $K_{abs}$ ) is obtained by simulation of Stokes flow with GeoDict.

### Capillary pressure vs. saturation relationship

In a second step, capillary pressure vs. saturation relationships are approximated with the PM method. The PM method [4], predicts the distribution of a wetting phase (WP) and a non-wetting phase (NWP) inside a porous medium. The method approximates drainage or imbibition by finding Young–Laplace equilibrium states through a series of morphological erosion and dilation operations using a spherical structuring element.

Here, primary drainage of the sample is computed. The drainage algorithm starts with a completely water-saturated porous medium and begins with a maximal pore radius  $R$ , which is then decreased step by step. In each step, a pore is drained if (i) the pore radius is larger than  $R$ , (ii) the entering non-wetting phase is connected by pores larger than  $R$  to the non-wetting phase reservoir, and (iii) the replaced wetting phase is connected to the wetting phase reservoir. Conditions (i) and (ii) describe the original algorithm as defined by [4] and used in [8]. Condition (iii) introduces a residual wetting phase and was added by [3].

The output of the algorithm is a finite sequence of quasi-stationary states. Each state is a 3D image again that encodes the solid phase(s), WP and NWP. In this study, the WP is a brine and the NWP an oil. In a post-processing step the Young-Laplace equation based on the radii of the inscribed spheres and the interfacial tension is used to predict the capillary pressure curve. The sequence of 3D images is then the input data to predict relative properties.

Most crucial for the calculations of the capillary pressure curve are the  $\theta$  of the fluid interfaces on the minerals present in the sample. Table 1 provides the  $\theta$  for the wetting phase used in the simulations. Realistic  $\theta$  for the present phases were not available in the literature and hence generic values are used that should illustrate the effect of different wettability on the transport properties. Generally, realistic  $\theta$  for individual minerals can be determined by experiments as described by [9, 10].

### Relative permeability

In a third step, the permeability for each fluid phase ( $K_w$ ,  $K_o$ ) in the Young–Laplace equilibrium states is computed by simulations of Stokes flow. These permeabilities are normalized with the corresponding  $K_{abs}$  yielding the relative permeabilities  $k_{r,w} = K_w / K_{abs}$  and  $k_{r,o} = K_o / K_{abs}$ .

## RESULTS

### Capillary pressure curves

The general shape of the capillary pressure curves exhibit differences in the capillary pressure required to maintain a certain water saturation ( $S_w$ ). In general, the simulation with multiple contact angles exhibits lower capillary pressures for a certain  $S_w$  in the sample especially for low  $S_w$  (Figure 2). The curves for primary drainage show further differences in the irreducible wetting phase saturation and displacement pressure. The irreducible wetting phase saturation is  $\sim 16\%$  for the run with constant  $\theta$  and  $\sim 10\%$  for the

run with multiple  $\theta$ . The displacement pressure is about 14 kPa for the constant  $\theta$  run and about 12 kPa for the multiple  $\theta$  run.

The capillary pressure curves exhibit an  $S_w$ -range ( $\sim 50\%$  -  $95\%$  for constant  $\theta$  and  $\sim 40\%$  -  $\sim 90\%$  for multiple  $\theta$ ) in which the PM method does not provide quasi-stationary states of the fluid distribution due to the structure of the pore space. In consequence, no  $k_r$  values could be computed in that range.

### Relative permeability

The  $k_r$  curves in Figure 3 are a combination of computed  $k_r$  values and  $k_r$  values derived from a Corey fit (see e.g. [1]). The Corey fits cover the above described  $S_w$ -range and are based on the computed  $k_r$  values.

The  $k_r$  curves for simulations with a constant  $\theta$  and multiple  $\theta$  show clear differences. The  $k_{r,w}$  curve for multiple  $\theta$  shows higher  $k_{r,w}$  values than the curve for constant  $\theta$  for similar  $S_w$ . Percolation of the WP stops for the Corey fits at  $S_w = 0.28$  (constant  $\theta$ ) and  $S_w = 0.09$  (multiple  $\theta$ ). The  $k_{r,o}$  curve for the multiple  $\theta$  displays lower  $k_{r,o}$  values for similar  $S_w$  in comparison with the constant  $\theta$  curve. Percolation of the NWP starts for the Corey fits at  $S_w = 0.79$  (constant  $\theta$ ) and  $S_w = 0.72$  (multiple  $\theta$ ).

However, the most striking feature is the difference in the crossover points between  $k_{r,w}$  and  $k_{r,o}$  which lie at  $S_w = 0.65$  for the constant  $\theta$  case and  $S_w = 0.57$  for the multiple  $\theta$  case. The crossover point between  $k_{r,w}$  and  $k_{r,o}$  is a good first indicator for the amount of recoverable oil [1]. The difference between the two crossover points is significant and non-consideration of multiple  $\theta$  may shift this point to artificially high  $S_w$  values. In order to avoid such effects, multiple  $\theta$  should be considered in digital rock physics workflows.

### REFERENCES

- [1] Berg, S, Rücker, M, Ott, H, Georgiadis, A, van der Linder, H, Enzmann, F, Kersten, M, Armstrong, R, de With, S, Becker, J, Wiegmann, A, “Connected pathway relative permeability from pore-scale imaging of imbibition”, *Adv Water Resour*, (2016) 90, 24–35 .
- [2] Blunt, MJ, Jackson, MD, Piri, M, Valvatne, PH, “Detailed physics, predictive capabilities and macroscopic consequences for pore-network models of multiphase flow”, *Adv Water Resour*, (2002) 25, 1069–89.
- [3] Ahrenholz, B, Tölke, J, Lehmann, P, Peters, A, Kaestner, A, Krafczyk, M, Durner, W, “Prediction of capillary hysteresis in a porous material using lattice-Boltzmann methods and comparison to experimental data and a morphological pore network model”, *Adv Water Resour*, (2008) 31, 1151–73.
- [4] Hilpert, M, Miller, TC, “Pore-morphology-based simulation of drainage in totally wetting porous media”, *Adv Water Resour*, (2001) 24, 243–55.

- [5] Silin, D, Tomutsa, L, Benson, S, Patzek, TW, “Microtomography and pore-scale modeling of two-phase fluid distribution”, *Transp Porous Media*, (2010) 86, 495–515.
- [6] Schulz, V, Wargo, E, Kumbur, E, “Pore-Morphology-Based Simulation of Drainage in Porous Media Featuring a Locally Variable Contact Angle”, *Transp Porous Media*, (2015) 107, 13-25.
- [7] Andrä, H, Combaret, N, Dvorkin, J, Glatt, E, Junehee, H, Kabel, M, Keehm, Y, Krzikalla, F, Lee, M, Madonna, C, Marsh, M, Mukerji, T, Saenger, E, Sain, R, Saxena, N, Ricker, S, Wiegmann, A, Zhan, A, “Digital rock physics benchmarks Part I: Imaging and segmentation”, *Computers & Geosciences*, (2013) 43, 25-32.
- [8] Becker, J, Schulz, V, Wiegmann, A, “Numerical determination of two-phase material parameters of a gas diffusion layer using tomography images”, *J Fuel Cell Sci Technol*, (2008) 5, 2, 21006-21014.
- [9] Brown, K, Schlüter, S, Sheppard, A, Wildenschild, D, “On the challenges of measuring interfacial characteristics of three-phase fluid flow with x-ray microtomography”, *J Microsc*, (2014) 253, 3, 171-182.
- [10] Andrew, M, Bijeljic, B, Blunt M, “Pore-scale contact angle measurements at reservoir conditions using X-ray microtomography” *Adv Water Resour*, (2014) 68, 24–31.

**Table 1.** Mineral phases and their associated contact angles to the wetting phase

Mineral phase	Constant contact angle [°]	Multiple contact angles [°]	Volume percentage [%]
Quartz	10	10	70.64
Feldspar	10	70	8.05
Ankerite	10	40	1.58
Zircon	10	60	0.14

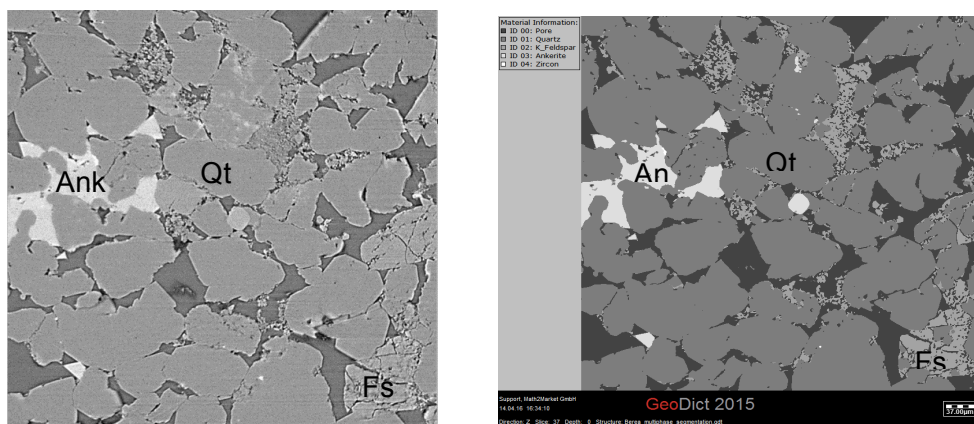


**Figure 1.** 2D illustration of the Berea sandstone. Qtz: quartz, Fsp: feldspar, Ank: ankerite. Left: XCT raw data. Mineral identification according to [7] and references therein. Right: Segmented data set.

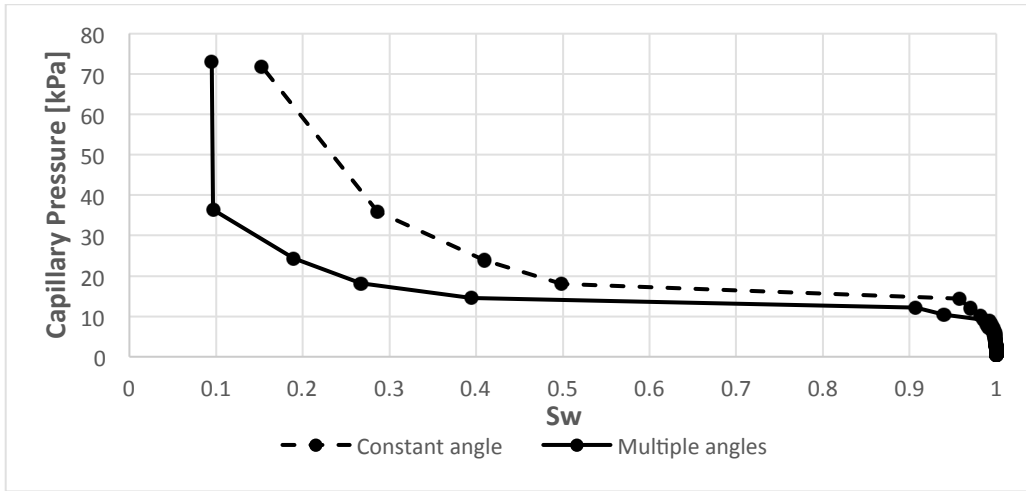


**Figure 2.** Capillary pressure curves for primary drainage in the Berea sandstone. Dashed line: simulation with a constant contact angle for all minerals. Continuous line: simulation with multiple contact angles.

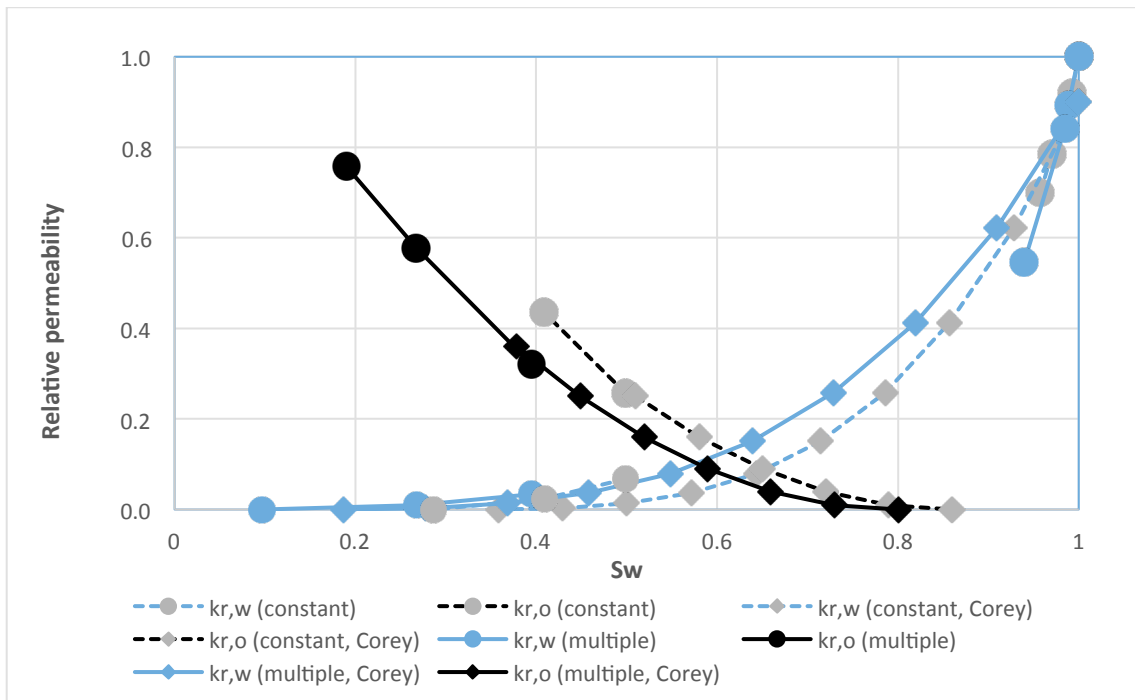


**Figure 3.** Relative permeability curves for primary drainage in the Berea sandstone. Simulations with a constant contact angle (dashed line) and with multiple contact angles (continuous line).